A comparative kinetic study of ethylene polymerization mediated by iron, cobalt and chromium catalysts bearing the same *N,N,N*-bis(imino)trihydroquinoline

Chuanbing Huang,[a,b,c,d] Vladimir A. Zakharov,*[c,d] Nina V. Semikolenova,[c] Mikhail A. Matsko,*[c] Gregory A. Solan,*[a,e] and Wen-Hua Sun*[a,b]

[a] Key Laboratory of Engineering Plastics and Beijing National Laboratory for Molecular Sciences, Institute of Chemistry, Chinese Academy of Sciences, Beijing 100190, China. E-mail: whsun@iccas.ac.cn

[b] CAS Research/Education Center for Excellence in Molecular Sciences, University of Chinese Academy of Sciences, Beijing 100049, China.

[c] Boreskov Institute of Catalysis, Pr. Lavrentieva 5, Novosibirsk 630090, Russian Federation. E-mail: zva@catalysis.ru or matsko@catalysis.ru

[d] Novosibirsk State University, Pirogova, 2, Novosibirsk 630090, Russian Federation.

[e] Department of Chemistry, University of Leicester, University Road, Leicester LE1 7RH, UK. E-mail: gas8@le.ac.uk

Abstract

The iron(II), cobalt(II) and chromium(III) chlorides, [2-{(2,4,6-Me$_3$C$_6$H$_2$)NCMe}-8-{N(2,4,6-Me$_3$C$_6$H$_2$)}C$_9$H$_8$N]MCl$_n$ (n = 2, M = Fe **LFeCl$_2$**, Co **LCoCl$_2$**; n = 3, M = Cr **LCrCl$_3$**), each bearing the same *N,N,N*-bis(imino)trihydroquinoline chelating ligand, have been employed as precatalysts for ethylene polymerization with modified methylaluminoxane (MMAO) as the co-catalyst. The kinetic profiles for these homogeneous polymerizations are reported in addition to the properties of the resultant polymers under comparable reaction conditions. All the experimental data indicate that the active metal center plays a key role on the catalytic performances of the complexes, especially the polymerization activity, thermal stability and lifetime of the active species. Under optimized conditions the iron catalyst displays the highest rate of polymerization but displays this for only a short period, while the chromium catalyst shows a lower maximum polymerization rate but sustains its performance over a longer period and at a higher temperature. In terms of the polymer properties, all three metal catalysts afford highly linear polymers with the metal center influencing the molecular weight and type of end group. Specifically, the cobalt and chromium catalysts produce narrowly dispersed low molecular weight polymers incorporating vinyl end groups, while the iron catalyst affords polymers of higher molecular weight displaying broad molecular weight distribution, with both saturated and unsaturated chain ends.

Keywords: 2-[1-(arylimino)ethyl]-8-arylimino-5,6,7-trihydroquinoline; cobalt; iron; chromium; kinetic data; ethylene polymerization.

1. Introduction

The use of 2,6-bis(imino)pyridine-metal(II) (metal = Fe, Co) chlorides as effective precatalysts for the polymerization of ethylene to highly linear polyethylenes has been the subject of on-going attention in academic circles since their introduction towards the end of the 1990's [1-9]. Indeed, a raft of studies have been conducted, aimed at elucidating the nature of catalytically active sites [10-18], while other metals centers such as vanadium and chromium have also emerged as polymerization-active for this class of ligand [19-25].
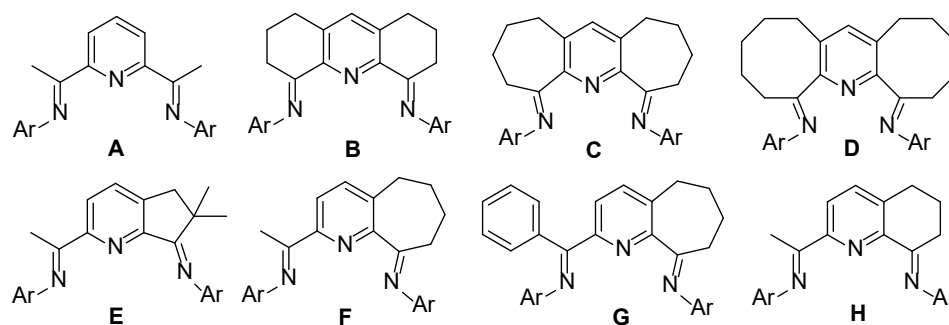

Chart 1 Fused ligand frameworks, **B – H**, derived from bis(imino)pyridine **A**

With the aim to fine tune the catalytic performances of such homogeneous catalysts and improve the properties of the polymeric products, much effort has been directed towards the design of novel *N,N,N*-ligands including the development of frameworks based on the fusion of cycloalkyl groups to the central pyridine ring in a 2,6-bis(imino)pyridine (**A**, Chart 1) [26]. For example, doubly fused bis(imino)pyridines such as 1,8-diimino-2,3,4,5,6,7-hexahydroacridine (**B**, Chart 1) [27], *α,α′*-bis(arylimino)-2,3:5,6-bis(pentamethylene)pyridine (**C**, Chart 1) [28-31] and *α,α′*-bis(arylimino)-2,3:5,6-bis(hexamethylene)pyridine (**D**, Chart 1) have all been reported [32]. In addition, unsymmetrical derivatives generated from the fusion of one cycloalkyl unit to the central pyridine donor in **A**, including 2-[1-(arylimino)ethyl]-7-arylimino-6,6-dimethylcyclopentapyridines (**E**, Chart 1) [33,34], 2-[1-(arylimino)ethyl]-9-arylimino-5,6,7,8-tetrahydrocycloheptapyridines (**F**, Chart 1) [35,36], 2-[1-(arylimino)benzylidene]-9-arylimino-5,6,7,8-tetrahydrocycloheptapyridines (**G**, Chart 1) [37-39] and 2-[1-(arylimino)ethyl]-8-arylimino-5,6,7-trihydroquinolines (**H**, Chart 1) have also been investigated [40-42]. Indeed, the performance of their resulting iron, cobalt and chromium catalysts has seen some notable differences when compared to their **A**-containing counterparts, including on catalytic activity, thermal stability as well as polymer molecular weight and dispersity. However, variations in the conditions of the polymerizations (*e.g.*, pressure, temperature, solvent, type and

amount of co-catalyst) employed to evaluate the effectiveness of such fused-ligand catalysts can sometimes limit a valid comparison especially when different metal centers are involved [26,43,44].

In this article, we re-examine under comparable conditions the catalytic performance of iron(II), cobalt(II) and chromium(III) complexes bearing the same cyclohexyl-fused ligand **H** as precatalysts for ethylene polymerization. We were drawn to this particular class of ligand due to the relative ease of synthesis and the quite distinct catalytic performances that have been independently reported by these three metal centers [40-42]. In particular, we conduct an in-depth polymerization study of each metal catalyst in turn under related operating conditions and then compare their performances to allow a clearer understanding of the effects of the type of metal on their kinetic data, catalytic activities as well as on the microstructural properties of resulting polyethylenes.

2. Experimental Section

2.1 General considerations

All experiments were performed in sealed high-vacuum systems using break-seal techniques. Heptane was dried over molecular sieves (4 Å), purified by refluxing over sodium metal, distilled under dry argon and then degassed under reduced pressure. Methylaluminoxane (MMAO), modified with $Al(i-Bu)_3$, was obtained from Akzo Nobel Corp. (1.7 M solution in heptane). Commercial $Al(i-Bu)_3$ was purchased from Aldrich and used as a heptane solution (1.0 M). The 2-[1-(mesitylimino)ethyl]-8-mesitylimino-5,6,7-trihydroquinoline complexes, **LFeCl₂**, **LCoCl₂** and **LCrCl₃**, were prepared according to previously published procedures [40-42].

2.2 Polymerization studies

The ethylene polymerization runs were performed in a 0.3 L steel reactor. A sealed glass ampule containing the required amount of precatalyst was placed in the reactor. The reactor was heated at 80 °C under vacuum for 1 h, cooled to 25 °C and then charged with the solution of the co-catalyst (MMAO: 1.7 M in heptane) and heptane (70 mL). After the desired temperature and ethylene pressure had been reached, the reaction was commenced by breaking the ampule containing the precatalyst. For polymerizations requiring 1-hexene, this was introduced into the reactor at the beginning of the polymerization run. During the reaction, the stirring speed, the temperature and the ethylene pressure were kept constant by using an automatic computer-controlled system for the ethylene feed which

allowed the ethylene consumption to be recorded and provided the kinetic curve output both as a table and as a graph. After a prescribed time, the ethylene pressure in the reactor was vented and the solid polymer was separated and dried under ambient conditions to a constant weight. The detailed experimental conditions are given in the footnotes of the Tables.

2.3 Polyethylene characterization

GPC measurements were performed using a PL-220 high-temperature instrument equipped with a set of PL-gel Olexis columns. The following run conditions were used: 160 °C, flow rate of 1 cm^3/min and 1,2,4-trichlorobenzene as a solvent. Conventional calibration was made using PS standards and PE standards with a narrow molecular weight distribution. The structural properties of the polymers were analyzed using high temperature ^{13}C NMR spectroscopy. Typically, a polyethylene sample (80 – 100 mg) was dissolved in dichlorobenzene (3 mL) and their inverse gated ^{13}C NMR spectra recorded on a Bruker AVANCE 400 spectrometer at 100.613 MHz in 10 mm standard glass tubes at 99 – 100 °C. Operating conditions used: spectral width 24 kHz, spectrum accumulation frequency 0.1 – 0.06 Hz, number of transients 2000 – 3000 and 45° pulse at 13 μs. The data were accumulated with 64 K data points in the time domain. The chemical shifts were referenced to the -($\underline{C}H_2$)$_n$- peak of a linear polyethylene (δ 30.0). The content of terminal propyl groups was determined from the integral intensities of the ^{13}C signals at δ 13.6 (–CH$_2$CH$_2$$\underline{C}H_3$), 22.4 (–CH$_2$$\underline{C}H_2CH_3$) and 31.7 (–$\underline{C}H_2CH_2CH_3$). To determine the content of terminal vinyl groups the integral intensities of the ^{13}C signals at δ 113.7 (–CH$_2$CH=$\underline{C}$H$_2$), 138.6 (–CH$_2$$\underline{C}$H=CH$_2$) and 33.4 (–$\underline{C}H_2$CH=CH$_2$) were measured. The content of methyl and vinyl groups in high molecular weight polyethylene samples was measured using IR spectroscopy with a FTIR-8400S SIMADZU Fourier spectrometer [45,46].

3. Results and Discussion

3.1 Synthesis of the precatalysts

The three complexes, [2-{(2,4,6-Me$_3$C$_6$H$_2$)NCMe}-8-{N(2,4,6-Me$_3$C$_6$H$_2$)}C$_9$H$_8$N]MCl$_n$ (n = 2, M = Fe **LFeCl$_2$**, Co **LCoCl$_2$**; n = 3, M = Cr **LCrCl$_3$**), each bearing the same mesityl-containing *N,N,N* ligand, have been synthesized in good yield using methods described in the literature (Figure 1) [40-42].
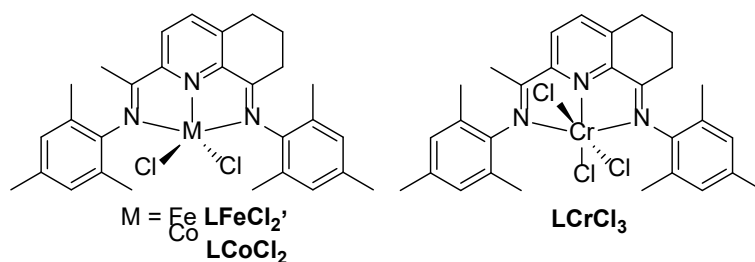
Chart 2 Iron, cobalt and chromium precatalysts to be investigated

3.2 Ethylene Polymerization Studies

The complexes, **LFeCl₂**, **LCoCl₂** and **LCrCl₃**, were screened as precatalysts for ethylene polymerization using modified methylaluminoxane (MMAO) as the co-catalyst. Each run was performed in heptane using optimized operating temperatures described in the literature and the rates of the polymerization recorded using an automatic computer-controlled ethylene feed monitoring system. The resulting polymers were characterized by gel permeation chromatography (GPC) and by a combination of NMR and IR spectroscopy.

(a) ***LFeCl₂/MMAO***. Using the optimum reaction temperature of 50 °C established in previous work for **LFeCl₂**/MMAO [40], with the ethylene pressure and run time fixed at 5 bar and 15 minutes, respectively, the effect of the Al:Fe molar ratio was initially examined; the results of the runs are summarized in Table 1 (entries 1 and 2) while the kinetic plots are displayed in Figure 1.

Table 1 Ethylene polymerization data obtained using **LFeCl₂**/MMAO[a]

Entry	PE (g)	Activity[b]	GPC (kg·mol⁻¹)			IR (content per 1000 C)[c]		Content per polymeric chain[c]	
			M_n	M_w	M_w/M_n	CH_3	$CH_2=CH$	CH_3	$CH_2=CH$
1	19.0	38.0	5.1	34.0	6.7	3.4	2.3	1.2	0.8
2[d]	11.6	23.2	11.5	43.5	3.8	1.5	1.6	1.2	1.3
3[e]	1.3	2.6	—	—	—	—	—	—	—
4[f]	6.1	3.1	2.6	190.0	73.1	4.5	1.7	0.8	0.3

[a] Conditions: 2 μmol of **LFeCl₂**, MMAO (Al:Fe = 1000), 5 bar of C_2H_4, 50 °C, 15 min, 100 mL of heptane;

[b] Average activity: × 10⁶ g PE (mol Fe)⁻¹ h⁻¹;

[c] Determined by FT-IR spectroscopy as polymer films;

[d] Al:Fe molar ratio = 500;

[e] 80 °C;

[f] Al(i-Bu)₃ as a co-catalyst (Al:Fe = 1000), 60 min.

On reducing the amount of MMAO from 1000 to 500 equivalents, the average activity decreased from 38.0×10^6 g PE (mol Fe)$^{-1}$ h^{-1} to 23.2×10^6 g PE (mol Fe)$^{-1}$ h^{-1} (entries 1 and 2, Table 1). Furthermore, the polymerization rate at the lower amount of co-catalyst was generally over the course of the run lower than that observed at 1000 (Figure 1). Even the period of very high activity observed at the start of the polymerization was noticeably shorter than that seen with larger amounts of co-catalyst. Hence, the stability of the active species and yield of polymer is strongly dependent on the amount of activator. With regard to the run performed at higher Al:Fe ratio, a very high initial activity of around 300×10^6 g PE (mol Fe)$^{-1}$ h^{-1} was observed which could be maintained for only about three minutes before rapidly declining and reaching a relatively stable level of 40×10^6 g PE (mol Fe)$^{-1}$ h^{-1} after about seven minutes. Increasing the reaction temperature to 80 °C and with the other parameters fixed [Al:Fe = 1000, P_{C2H4} = 5 bar], the average activity dramatically dropped to 2.6×10^6 g PE (mol Fe)$^{-1}$ h^{-1} affording only 1.3 g of isolable polymer. This observation indicates that the intermediates or active species produced using **LFeCl₂**/MMAO are very sensitive to the reaction temperature.

On substituting MMAO for Al(i-Bu)₃ as the co-catalyst, with the reaction temperature kept at 50 °C and the Al:Fe ratio at 1000, the average activity of **LFeCl₂**/Al(i-Bu)₃ lowered from 38.0×10^6 g PE (mol Fe)$^{-1}$ h^{-1} to 3.1×10^6 g PE (mol Fe)$^{-1}$ h^{-1} (entries 1 and 4, Table 1). This result indicates that Al(i-Bu)₃ is an inferior activator when compared to MMAO, which is in stark contrast to the previously reported high catalytic observed activity using a 2,6-bis(imino)pyridine-iron(II) complex activated with Al(i-Bu)₃ [43,44].
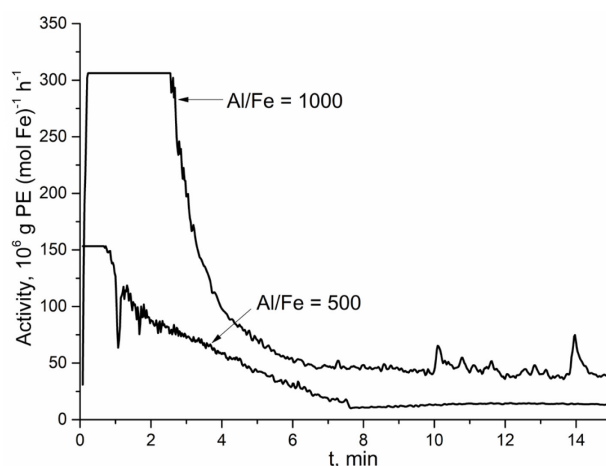

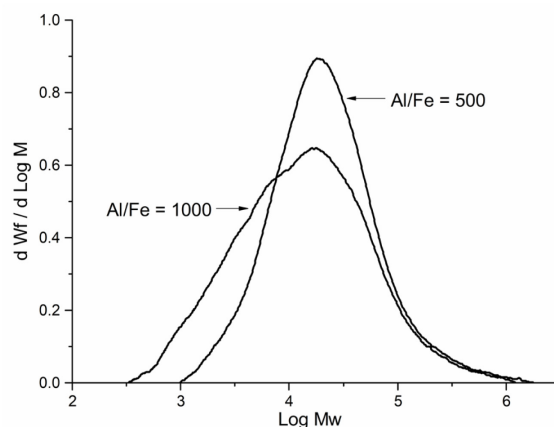**Figure 1** Ethylene polymerization rate *vs*. time for **LFeCl₂**/MMAO with two different amounts of co-catalyst

Figure 2 GPC curves for the polyethylenes generated using **FeCl₂**/MMAO with two different amounts of MMAO

In terms of the polymer properties, it was found that the weight-averaged molecular weight (M_w) and the molecular weight distribution (M_w/M_n) of the polyethylenes generated using **LFeCl₂**/MMAO were dependent on the amount of MMAO used (entries 1 and 2, Table 1). In particular, the M_w decreased slightly while the M_w/M_n values noticeably increased from 3.8 to 6.7 as the Al:Fe molar ratio was raised. Furthermore, a lower molecular weight shoulder peak could be observed in the GPC trace with the larger amount of MMAO (Figure 2). This broadening of the molecular weight distribution can be attributed to the onset of chain transfer to aluminum as a termination pathway leading to polymer with lower molecular weight [40]. Indeed, comparison of the ratios of terminal methyl to vinyl groups in the IR spectra of the corresponding polymers supports this assertion (entries 1 and 2, Table 1). At an Al:Fe ratio of 500, an approximate 1:1 ratio of the methyl to vinyl chain ends is seen which is consistent with β-H elimination/transfer to monomer as the predominant termination pathway. By contrast at an Al:Fe ratio of 1000, the 1.5:1 ratio of methyl to vinyl chain ends is observed, which implies that chain transfer aluminum is now competitive with β-H elimination.

In the case of the polymer formed using **LFeCl₂**/Al(i-Bu)₃ (entry 4, Table 1), the polyethylene exhibited a particularly broad molecular weight distribution (M_w/M_n = 73.1). Indeed, inspection of the GPC trace reveals a bimodal distribution with a very low molecular weight peak (M_{pk} = 0.65 kg·mol⁻¹) displaying a narrow molecular weight distribution (peak A, Figure 3) along with higher molecular weight peak (M_{pk} = 54 kg·mol⁻¹) exhibiting a broader molecular weight distribution (peak B, Figure 3). As with observations noted with different amounts of MMAO, it would seem likely that two different termination pathways are operative with Al(i-Bu)₃ as co-catalyst.
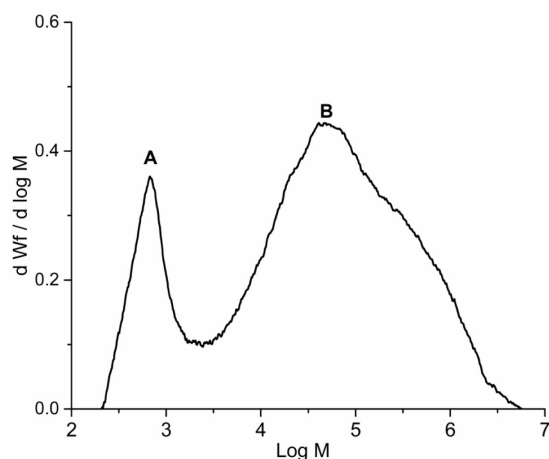
Figure 3 GPC curves for the polyethylene obtained using **LFeCl$_2$**/Al(i-Bu)$_3$

(b) **LCoCl$_2$/MMAO**. With the operating temperature set at 60 °C [41], the effect of pressure and amount of the **LCoCl$_2$**/MMAO catalyst was investigated with the Al:Co molar ratio and run time fixed at 1000 and 15 minutes, respectively; the results of the runs are compiled in Table 2 (entries 1 – 3) while the kinetic plots are displayed in Figure 4.

Table 2 Ethylene polymerization data obtained using **LCoCl$_2$**/MMAO[a]

Entry	T (°C)	PE (g)	Activity[b]	M_{pk}[c]	M_w[c]	M_w/M_n[c]	CH$_3$ per 1000 C[d]	CH$_2$=CH per 1000 C[d]
1	60	15.8	31.6	0.46	0.67	1.6	22.7	21.9
2[e]	60	26.6	53.2	0.55	0.72	1.4	—	—
3[f]	60	19.4	38.8	0.70	0.71	1.6	—	—
4	80	2.8	5.6	0.62	0.75	1.4	—	—

[a] Conditions: 2 μmol of **LCoCl$_2$**, MMAO (Al:Co = 1000), 5 bar C$_2$H$_4$, 60 °C, 100 mL of heptane, 15 min;

[b] Average activity: × 10^6 g PE (mol Co)$^{-1}$ h^{-1};

[c] M_{pk} and M_w: kg·mol^{-1}, determined by GPC;

[d] Determined by ^{13}C NMR spectroscopy;

[e] 10 bar C$_2$H$_4$;

[f] 1 μmol **LCoCl$_2$**, MMAO (Al:Co = 1000), 5 bar C$_2$H$_4$, 60 °C, 100 mL of heptane, 30 min.

On increasing the ethylene pressure from 5 to 10 bar, the average activity of **LCoCl$_2$**/MMAO rose from 31.6 × 10^6 g PE (mol Co)$^{-1}$ h^{-1} to 53.2 × 10^6 g PE (mol Co)$^{-1}$ h^{-1} (entries 1 and 2, Table 2) in accord with more efficient ethylene coordination and higher insertion rates at higher pressures [41]. At both pressures, a high initial polymerization rate (114 – 119 × 10^6 g PE (mol Co)$^{-1}$ h^{-1}) was followed by a sudden drop with the higher pressure run seeing a slightly more sustained period of high activity

(*ca.* 3 minutes). After 15 minutes the rate had begun to reach a plateau of 50×10^6 g PE (mol Co)$^{-1}$ h^{-1} at 10 bar and 30×10^6 g PE (mol Co)$^{-1}$ h^{-1} at 5 bar. On the other hand, decreasing the amount of **LCoCl₂** from 2 to 1 µmol, with the molar ratio of Al:Co kept at 1000 and the ethylene pressure at 5 bar, a maximum polymerization rate of about 100×10^6 g PE (mol Co)$^{-1}$ h^{-1}) was reached after two minutes before reducing steadily. Notably, the activity after about 3 minutes was higher than that seen with the larger amount of precatalyst (Figure 4). Moreover, the activity after 30 minutes with 1 µmol of precatalyst was of a comparable value to that observed after 15 minutes with 2 µmol of precatalyst highlighting the effects of catalyst concentration on rate and lifetime. With the polymerization temperature increased to 80 °C and the amount of precatalyst returned to 2 µmol (entry 4, Table 2), the average activity decreased by more than five-fold when compared with that observed at 60 °C, indicating the inferior stability of this cobalt catalyst at higher temperature.
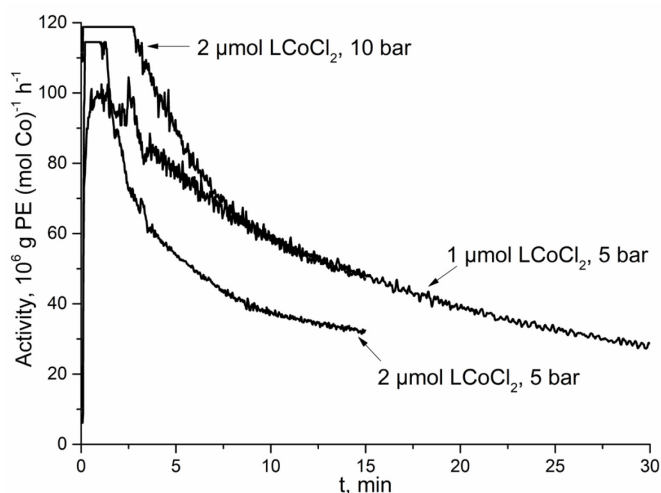

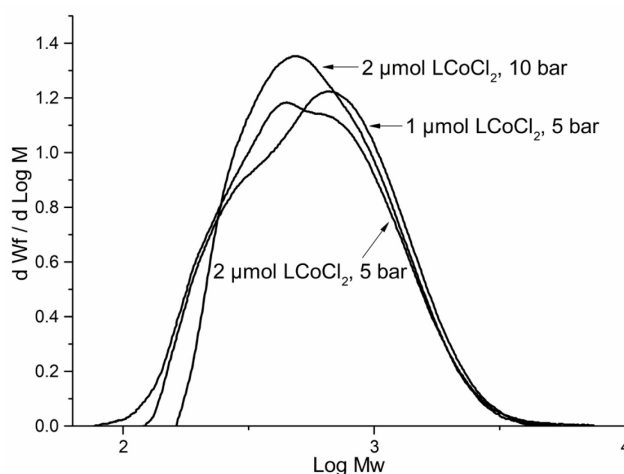**Figure 4** Ethylene polymerization rate *vs*. time for **LCoCl₂**/MMAO under different conditions

Figure 5 GPC curves for the polyethylenes obtained using **LCoCl₂**/MMAO under different conditions

As the molecular weights of the polymers obtained using **LCoCl₂**/MMAO were relatively low (M_w range: 0.67 – 0.75 kg·mol^{-1}), their GPC curves fell partly outside the range covered by conventional PS and PE calibration standards, a M_{pk} peak was used as a reference standard (Table 2). Nonetheless, a comparison of the GPC traces for the polymers obtained at different ethylene pressures, with the amount of precatalyst fixed, reveals a larger proportion of the low molecular weight fraction at lower pressure: M_{pk} of 0.46 kg·mol^{-1} at 5 bar versus 0.55 kg·mol^{-1} at 10 bar (Figure 5). Indeed, such pressure effects on molecular weight are consistent with observations noted previously [41].

To explore the microstructural properties of the polymers, a ^{13}C NMR spectrum was recorded of the polyethylene obtained using **LCoCl₂**/MMAO at 5 bar C_2H_4 (entry 1, Table 2). The spectrum revealed an intense signal at δ 30.0 along with less intense peaks corresponding to the -(CH₂)- repeat unit of a linear polymer (Figure 6). In addition, peaks could be assigned to propyl and vinyl end groups allowing the number of terminal methyl and vinyl groups to be determined as 22.7 and 21.9 per 1000 C, respectively. Furthermore, the number average molecular weight (M_n) was calculated as 0.62 kg·mol^{-1} which corresponds to 1.0 terminal methyl and 1.0 vinyl group per polyethylene chain [45].
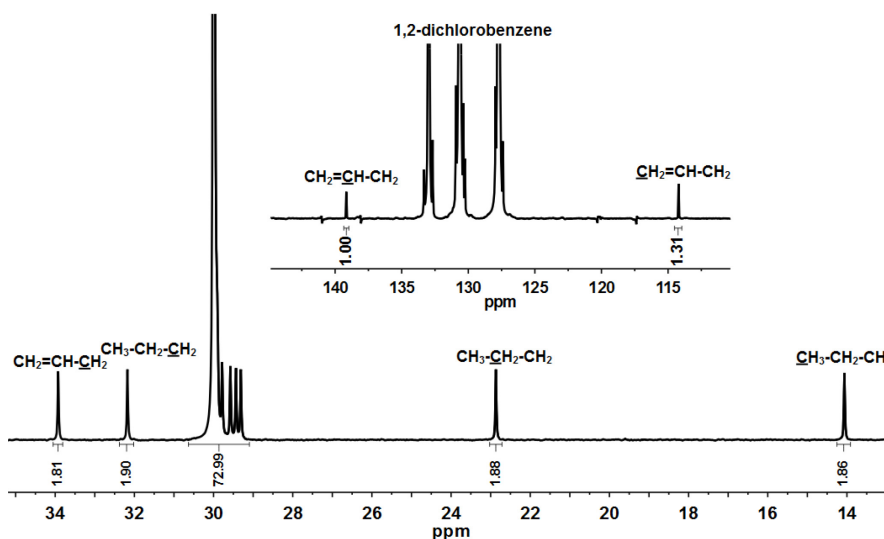

Figure 6 ^{13}C NMR spectrum of the polyethylene obtained by **LCoCl₂**/MMAO (entry 2, Table 2)

(c) ***LCrCl₃/MMAO***. Based on the optimum reaction temperature determined elsewhere as 80 °C [42], the performance of **LCrCl₃**/MMAO was studied in the first instance over a range of Al:Cr molar ratios with the ethylene pressure maintained at 5 bar; the results of the polymerization runs are collected in Table 3 (entries 1 – 3).

Table 3 Ethylene polymerization data obtained using **LCrCl₃**/MMAO[a]

Entry	Al:Cr	t (min)	PE (g)	Activity[b]	M_{pk}[c]	M_w[c]	M_w/M_n[c]	CH₃ per 1000 C[d]	CH₂=CH per 1000 C[d]
1	2000	60	58.3	29.2	0.73	0.75	1.6	—	—
2	1000	30	75.1	75.1	0.75	0.76	1.7	16.2	15.7
3	500	30	26.4	26.4	0.72	0.77	1.7	—	—
4[e]	1000	15	3.6	7.2	0.68	0.63	1.3	—	—
5[f]	1000	10	11.0	33.0	0.48	0.61	1.5	24.5	24.4

[a] Conditions: 2 μmol of **LCrCl₃**, MMAO, 5 bar C₂H₄, 80 °C, 100 mL of heptane;

[b] Average activity: × 10⁶ g PE (mol Cr)⁻¹ h⁻¹;

[c] M_{pk} and M_w: kg·mol⁻¹, determined by GPC;

[d] Determined by ¹³C NMR spectroscopy;

[e] 50 °C;

[f] + 15 mL of 1-hexene.

On varying the Al:Cr molar ratio of **LCrCl₃**/MMAO from 2000 to 500, the highest average activity of 75.1 × 10⁶ g PE (mol Cr)⁻¹ h⁻¹ was achieved after 30 minutes with a ratio of 1000 (entry 2, Table 3). Either increasing the ratio up to 2000 or decreasing it to 500 led to a marked decrease of activity (entries 1 – 3, Table 3). In common to all the molar ratios examined, a similar shape for the kinetic curves was observed (Figure 7), with a clear induction period occurring in each case whereby the highest polymerization rate was reached after periods of between 8 – 15 minutes and then steadily decreased over more extended run times. Notably, this decrease of the polymerization rate from its maximum (R_p^{max}) to its value after 30 minutes (R_p^{30}) was found to be dependent on the Al:Cr molar ratio with the ratio of $R_p^{max}:R_p^{30}$ increasing from 1.8 (Al:Cr = 2000) to 4.0 (Al:Cr = 500).

The effect of temperature on the polymerization using **LCrCl₃**/MMAO was also explored. By changing it from 80 to 50 °C under otherwise identical conditions (Al:Cr = 1000, entries 2 and 4, Table 3), the average activity of dropped from 75.1 × 10⁶ g PE (mol Cr)⁻¹ h⁻¹ at 80 °C to 7.2 × 10⁶ g PE (mol Cr)⁻¹ h⁻¹ at 50 °C highlighting the preferred high operating temperature of this chromium catalyst. To examine the effect of α-olefin addition, 1-hexene was introduced (1-hexene:ethylene = 2:1) to the polymerization with the Al:Cr molar ratio kept at 1000 (entry 5, Table 3). A noticeable decrease in activity (*ca.* 2.3 times) was observed but with the effect of producing a more stable activity profile (Figure 7).
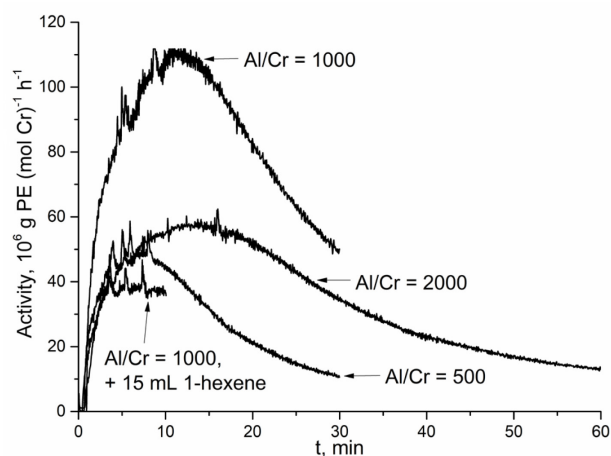
Figure 7 Ethylene polymerization rate *vs.* time for **LCrCl₃**/MMAO system under different conditions

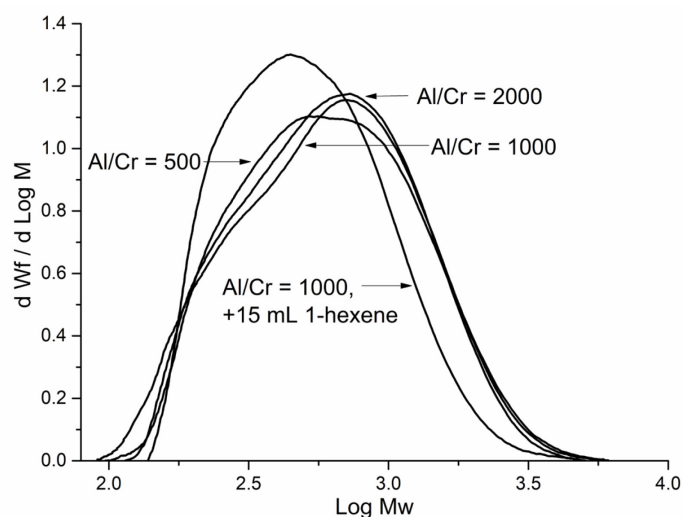**Figure 8** GPC curves of the polyethylenes obtained using **LCrCl₃**/MMAO at different Al:Cr molar ratios and with the introduction of 1-hexene

Due to the low molecular weight of the polymers obtained using **LCrCl₃**/MMAO and their incompatibility with the PS and PE calibration standards, a M_{pk} peak was again used as a reference standard in a manner similar to that described for the polymers generated using **LCoCl₂**/MMAO. Unlike with the observations noted with polymerization activity, the amount of co-catalyst (Al:Cr ratio) had little effect on the molecular weight of the polymers (M_w range: 0.75 – 0.77 kg·mol⁻¹; entries 1 – 3, Table 3). Likewise, little variation in the molecular weight distributions was observed over the range of molar ratios, as well as reaction times, with narrow polydispersities remaining a general feature (M_w/M_n = 1.5 – 1.7, Figure 8). The ¹³C NMR spectrum of the polymer sample obtaining using the most active chromium catalyst (entry 2, Table 3), revealed a highly linear polymer that contained 16.2 terminal methyls and 15.7 vinyl groups per 1000 C (Figure 9). Based on the relative integrals [45], the

number average molecular weight (M_n) of this polymer was determined as 0.87 kg·mol^{-1} with 1.0 terminal methyl and 1.0 vinyl groups per polyethylene chain.

With regard to the polymer generated following 1-hexene addition, the effect of it presence was to reduce the molecular weight (entry 5, Table 3). Indeed, the ^{13}C NMR spectrum revealed 24.5 terminal methyls and 24.4 vinyl groups per 1000 C (Figure 10). The M_n value was determined as 0.57 kg·mol^{-1} which corresponds to 1.0 terminal methyl and 1.0 vinyl group per polymeric chain. Moreover, peaks for n-butyl branches were detected in the ^{13}C NMR spectrum, with a value of 2.2 n-butyl groups per 1000 C based on their relative integrals [45], indicating a very low incorporation of 1-hexene into polyethylene chain. Overall, it would appear that the main role of the 1-hexene in this polymerization is to act as a chain transfer agent leading to a decrease in the polymer molecular weight (Figure 8) [43].
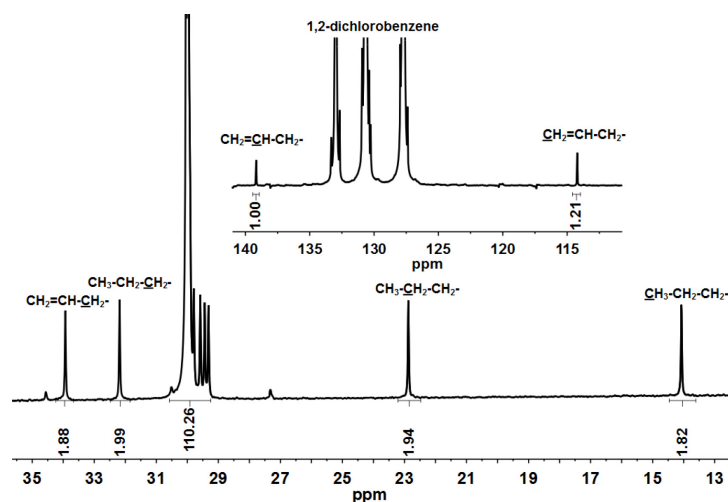

Figure 9 ^{13}C NMR spectrum of the polyethylene obtained using **LCrCl₃**/MMAO (entry 2, Table 3)

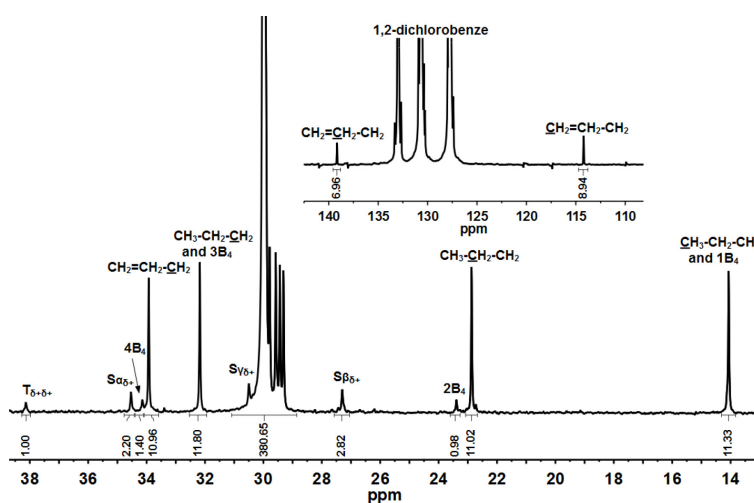**Figure 10** ^{13}C NMR spectrum of the copolymer obtained using **LCrCl₃**/MMAO (entry 5, Table 3)

13

3.3 Comparison of the catalytic performance of the iron, cobalt and chromium catalysts

With the main aim of this work to compare the performance of these iron, cobalt and chromium catalysts, key kinetic and GPC data for the corresponding polymers extracted from Tables 1 – 3 are summarized in Table 4; Figures 11 and 12 depict their relative kinetic and GPC profiles.

Table 4 Comparative data for the iron, cobalt and chromium catalysts tested at optimal polymerization temperatures

Entry	Precatalyst	T (°C)[a]	R_p^{max} [b]	R_p^{15} [c]	M_w (kg·mol^{-1})	M_w/M_n
2 (Table 1)	**LFeCl$_2$**	50	300	40	43.5	3.8
2 (Table 2)	**LCoCl$_2$**	60	115	30	0.67	1.6
2 (Table 3)	**LCrCl$_3$**	80	115	105	0.76	1.7

[a] Polymerization temperature;

[b] Maximum polymerization rate: $\times 10^6$ g PE (mol M)$^{-1}$ h^{-1};

[c] Polymerization rate after 15 min: $\times 10^6$ g PE (mol M)$^{-1}$ h^{-1}.

The iron catalyst showed an exceptionally high activity of 300×10^6 g PE (mol Fe)$^{-1}$ h^{-1} over the first three minutes of the polymerization, after which this rate rapidly decreased to 50×10^6 g PE (mol Fe)$^{-1}$ h^{-1} at the six minute mark and then remained relatively stable at 40×10^6 g PE (mol Fe)$^{-1}$ h^{-1} for the remainder of the run. In comparison, the cobalt catalyst displayed an initial activity of 115×10^6 g PE (mol Co)$^{-1}$ h^{-1} and maintained this level for about two minutes, before dropping to a value of 30×10^6 g PE (mol Co)$^{-1}$ h^{-1} after 15 minutes. Hence, both the iron and cobalt catalysts showed their maximum activity at the start of the polymerization (less than 3 minutes) with the iron system displaying more than double the value exhibited by the cobalt system but then levelling off to a comparable lower level after 15 minutes. On the other hand, the chromium catalyst displayed a noticeable induction period in which the rate of polymerization initially accelerated reaching a maximum value of 115×10^6 g PE (mol Cr)$^{-1}$ h^{-1} after 10 minutes. The polymerization rate then remained relatively stable over the next 5 minutes and then gradually reduced. Indeed, after thirty minutes, the activity declined to only 60×10^6 g PE (mol Cr)$^{-1}$ h^{-1}, which is notably higher than that seen for both the iron and cobalt catalysts after 15 minutes. Hence, the chromium catalyst not only displays a longer period of induction but also shows a gentler deceleration in activity when compared with the iron and cobalt systems. In terms of the maximum catalytic activity, the value was found to fall in the order, R_p^{max} (**LFeCl$_2$**, 50 °C) > R_p^{max} (**LCoCl$_2$**, 60 °C) ≈ R_p^{max} (**LCrCl$_3$**, 80 °C) with the

duration of this high performance very short for **LFeCl₂** and **LCoCl₂** (2 – 3 minutes at 50 – 60 °C), while for **LCrCl₃** a more stable profile is observed and moreover at a higher temperature of 80 °C.
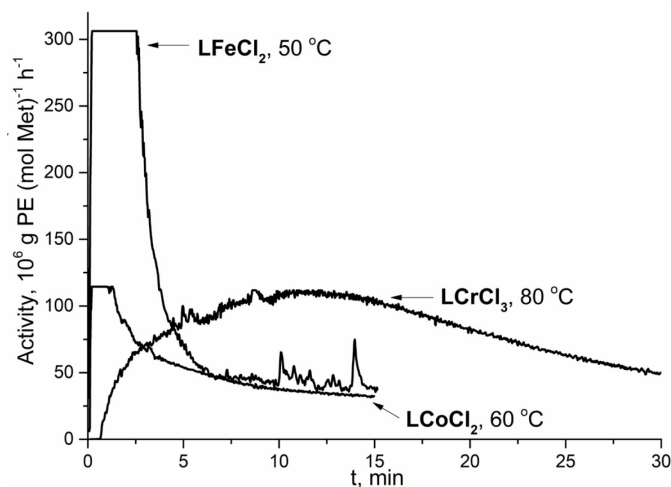

Figure 11 Polymerization rate *vs.* time for the three different metal complexes at their optimum reaction temperatures

With respect to the resulting polymers (Figure 12 and Table 4), the materials generated by the cobalt and chromium complexes showed very similar molecular weights (M_w range: 0.67 – 0.76 kg·mol^{-1}) and displayed comparable molecular weight distributions (M_w/M_n range: 1.6 – 1.7). Conversely, the polyethylenes produced by the iron catalyst exhibited much higher molecular weight ($M_w = 43.5$ kg·mol^{-1}) and showed a broader molecular weight distribution ($M_w/M_n = 3.8$).
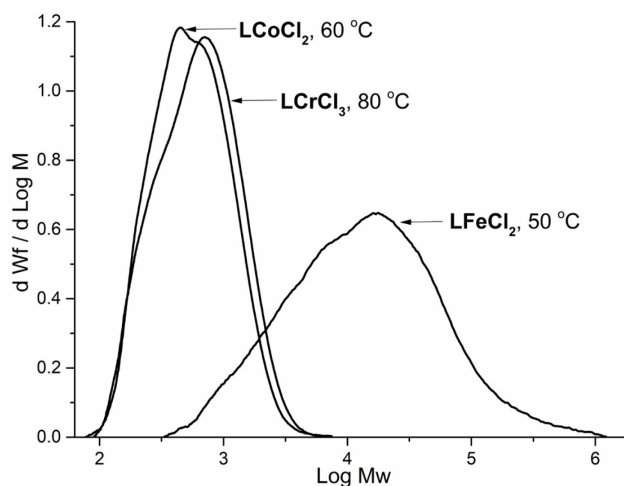

Figure 12 GPC curves for the polyethylenes obtained by the iron, cobalt and chromium catalysts at their optimum reaction temperatures

Based on the NMR data, a similar content of terminal methyl and vinyl groups for the polymers produced by the cobalt and chromium catalysts is apparent with essentially one methyl and one vinyl groups per polymer chain. In terms of termination pathway, it is apparent that β-hydride elimination or transfer to monomer operates as the dominant mechanism for both these catalysts. Additionally, it can be concluded that the ratio of the propagation to the termination rate constants (k_p/k_t) is also similar for

both systems due to the comparable values of the molecular weight of the polymers produced. However, the key difference between these two catalysts is that the chromium catalyst has shown much greater thermal stability. On the other hand, the performance of the iron catalyst was markedly different from that observed using the cobalt and chromium catalysts. Notably, **LFeCl₂**/MMAO (i) produced polyethylene with much higher molecular weight and broader molecular weight distribution with an increase in the Al:Fe molar ratio, and (ii) exhibited a much higher initial maximum catalytic activity in comparison with **LCoCl₂**/MMAO and **LCrCl₃**/MMAO, but showed the least thermal stability. In addition, the rate of polymerization after 15 minutes for **LFeCl₂**/MMAO was lower in comparison with that of **LCrCl₃**/MMAO. As a general point, these *N,N,N*-bis(imino)trihydroquinoline catalysts, when put alongside their 2,6-bis(imino)pyridine-M (M = Fe, Co, Cr) counterparts, exhibit better thermostability and the resultant polymers display lower molecular weights with narrower distributions [41,42], an observation that could be attributed to the presence of the cyclohexyl-fused pyridine framework [26]. Moreover, the kinetic profiles of the current catalysts show some differences when compared with the corresponding bis(imino)pyridine systems, especially for the chromium catalysts which displays a notably shorter induction period [43].

4. Conclusions

A kinetic investigation involving the use of three structurally related iron, cobalt and chromium precatalysts, **LFeCl₂**, **LCoCl₂** and **LCrCl₃**, for the polymerization of ethylene has been undertaken under a set of closely related conditions. With MMAO as the co-catalyst in each case, the resulting catalytic performance has been shown to be strongly dependent on the transition metal center employed. **LFeCl₂**/MMAO has demonstrated a very high initial activity at a relatively low polymerization temperature (50 °C) but displayed this high activity only over a short duration. In comparison, **LCoCl₂**/MMAO revealed a lower optimal polymerization activity and showed this over a slightly shorter time but exhibited similar stability. On the other hand, **LCrCl₃**/MMAO, despite having a maximum catalytic activity comparable with that observed for cobalt, had a longer induction period and a more sustained level of good activity. Moreover, the chromium catalyst displayed these simpler performance characteristics at a higher temperature (80 °C). All three catalysts generated linear polyethylene with the chromium and cobalt systems forming narrowly dispersed lower molecular weight material while the iron catalyst afforded higher molecular weight material with a broader

distribution. Overall, the more straightforward kinetic profile exhibited by the chromium catalyst coupled with its selectivity for vinyl-terminated polymeric waxes, offers considerable potential for industrial development.

Acknowledgements

References

[1] B.L. Small, M. Brookhart, A.M.A. Bennett, J. Am. Chem. Soc. 120 (1998) 4049–4050.

[2] G.J.P. Britovsek, V.C. Gibson, B.S. Kimberley, P.J. Maddox, S.J. McTavish, G.A. Solan, A.J.P. White, D.J. Williams, Chem. Commun. 7 (1998) 849–850.

[3] B.L. Small, M. Brookhart, J. Am. Chem. Soc. 120 (1998) 7143–7144.

[4] G.J.P. Britovsek, M. Bruce, V.C. Gibson, B.S. Kimberley, P.J. Maddox, S. Mastroianni, S.J. McTavish, C. Redshaw, G.A. Solan, S. Strömberg, A.J.P. White, D.J. Williams, J. Am. Chem. Soc. 122 (1999) 8728–8740.

[5] G.J.P. Britovsek, S. Mastroianni, G.A. Solan, S.P.D. Baugh, C. Redshaw, V.C. Gibson, A.J.P. White, D.J. Williams, M.R.J. Elsegood, Chem. Eur. J. 6 (2000) 2221–2231.

[6] V.C. Gibson, C. Redshaw, G.A. Solan, Chem. Rev. 107 (2007) 1745–1776.

[7] Q. Mahmood, J. Guo, W. Zhang, Y. Ma, T. Liang, W.-H. Sun, Organometallics 37 (2018) 957–970.

[8] V.C. Gibson, G.A. Solan, Top. Organomet. Chem. 26 (2009) 107–158.

[9] V.C. Gibson, G.A. Solan, in Catalysis without Precious Metals (Ed. R. M. Bullock), Wiley-VCH, Weinheim, (2010) 111–141.

[10] G.J.P. Britovsek, G.K.B. Clentsmith, V.C. Gibson, D.M.L. Goodgame, S.J. McTavish, Q.A. Pankhurst, Catal. Commun. 3 (2002) 207−211.

[11] K.P. Bryliakov, N.V. Semikolenova, V.A. Zakharov, E.P. Talsi, Organometallics 23 (2004) 5375−5378.

[12] K.P. Bryliakov, N.V. Semikolenova, V.N. Zudin, V.A. Zakharov, E.P. Talsi, Catal. Commun. 5 (2004) 45−48.

[13] V.L. Cruz, J. Ramos, J. Martínez-Salazar, S. Gutiérrez-Oliva, A. Toro-Labbé, Organometallics 28 (2009) 5889−5895.

[14] R. Raucoules, T. de Bruin, P. Raybaud, C. Adamo, Organometallics 28 (2009) 5358−5367.

[15] K.P. Bryliakov, E.P. Talsi, N.V. Semikolenova, V.A. Zakharov, Organometallics 28 (2009) 3225−3232.

[16] A.M. Tondreau, C. Milsmann, A.D. Patrick, H.M. Hoyt, E. Lobkovsky, K. Wieghardt, P.J. Chirik, J. Am. Chem. Soc. 132 (2010) 15046−15059.

[17] A.A. Barabanov, G.D. Bukatov, V.A. Zakharov, N.V. Semikolenova, T.B. Mikenas, L.G. Echevskaja, M.A. Matsko, Macromol. Chem. Phys. 207 (2006) 1368–1375.

[18] A.A. Barabanov, G.D. Bukatov, V.A. Zakharov, N.V. Semikolenova, L.G. Echevskaja, M.A. Matsko, Macromol. Chem. Phys. 209 (2008) 2510–2515.

[19] D. Reardon, F. Conan, S. Gambarotta, G. Yap, Q. Wang, J. Am. Chem. Soc. 121 (1999) 9318–9325.

[20] M.A. Esteruelas, A.M. López, L. Méndez, M. Oliván, E. Oñate, Organometallics 22 (2003) 395–406.

[21] Y. Nakayama, K. Sogo, H. Yashida, T. Shiono, J. Polym. Sci. Part A: Polym. Chem. 43 (2005) 3368–3375.

[22] B.L. Small, M.J. Carney, D.M. Holman, C.E. O'Rourke, J.A. Halfen, Macromolecules 37 (2004) 4375–4386.

[23] I.E. Soshnikov, N.V. Semikolenova, A.A. Antonov, K.P. Bryliakov, V.A. Zakharov, E.P. Talsi, Organometallics 33 (2014) 2583−2587.

[24] I.E. Soshnikov, N.V. Semikolenova, K.P. Bryliakov, V.A. Zakharov, E.P. Talsi, ChemCatChem 9 (2017) 1253–1260.

[25] I.E. Soshnikov, N.V. Semikolenova, K.P. Bryliakov, V.A. Zakharov, E.P. Talsi, J. Organomet. Chem. 867 (2018) 4–13.

[26] Z. Wang, G.A. Solan, W. Zhang, W.-H. Sun, Coord. Chem. Rev. 363 (2018) 92–108.

[27] V.K. Appukuttan, Y. Liu, B.C. Son, C.-S. Ha, H. Suh, I. Kim, Organometallics 30 (2011) 2285–2294.

[28] S. Du, W. Zhang, E. Yue, F. Huang, T. Liang, W.-H. Sun, Eur. J. Inorg. Chem. (2016)1748–1755.

[29] S. Du, X. Wang, W. Zhang, Z. Flisak, Y. Sun, W.-H. Sun, Polym. Chem. 7 (2016) 4188–4197.

[30] C. Huang, S. Du, G.A. Solan, Y. Sun, W.-H. Sun, Dalton Trans. 46 (2017) 6948–6957.

[31] H. Suo, I.I. Oleynik, C. Bariashir, I.V. Oleynik, Z. Wang, G.A. Solan, Y. Ma, T. Liang, W.-H. Sun, Polymer 149 (2018) 45–54.

[32] Z. Wang, G.A. Solan, Q. Mahmood, Q. Liu, Y. Ma, X. Hao, W.-H. Sun, Organometallics 37 (2018) 380–389.

[33] J. Ba, S. Du, E. Yue, X. Hu, Z. Flisak, W.-H. Sun, RSC Adv. 5 (2015) 32720–32729.

[34] Y. Zhang, C. Huang, X. Hao, X. Hu, W.-H. Sun, RSC Adv. 6 (2016) 91401–91408.

[35] F. Huang, Q. Xing, T. Liang, Z. Flisak, B. Ye, X. Hu, W. Yang, W.-H. Sun, Dalton Trans. 43 (2014) 16818–16829.

[36] F. Huang, W. Zhang, E. Yue, T. Liang, X. Hu, W.-H. Sun, Dalton Trans. 45 (2016) 657–666.

[37] F. Huang, W. Zhang, Y. Sun, X. Hu, G.A. Solan, W.-H. Sun, New J. Chem. 40 (2016) 8012–8023.

[38] Y. Zhang, H. Suo, F. Huang, T. Liang, X. Hu, W.-H. Sun, J. Polym. Sci. Part A: Polym. Chem. 55 (2017) 830–842.

[39] C. Huang, Y. Huang, Y. Ma, G.A. Solan, Y. Sun, X. Hu, W.-H. Sun, Dalton Trans. 47 (2018) 13487–13497.

[40] W. Zhang, W. Chai, W.-H. Sun, X. Hu, C. Redshaw, X. Hao, Organometallics 31 (2012) 5039–5048.

[41] W.-H. Sun, S. Kong, W. Chai, T. Shiono, C. Redshaw, X. Hu, C. Guo, X. Hao, Appl. Catal. A: Gen. 447–448 (2012) 67–73.

[42] C. Huang, Y. Zhang, G.A. Solan, Y. Ma, X. Hu, Y. Sun, W.-H. Sun, Eur. J. Inorg. Chem. (2017) 4158–4166.

[43] N.V. Semikolenova, V.A. Zakharov, L.G. Echevskaja, M.A. Matsko, K.P. Bryliakov, E.P. Talsi, Catal. Today 144 (2009) 334–340.

[44] N.V. Semikolenova, V.A. Zakharov, E.P. Talsi, D.E. Babushkin, A.P. Sobolev, L.G. Echevskaya, M.M. Khysniyarov, J. Mol. Catal. A: Chem. 182–183 (2002) 283–294.

[45] L.G. Echevskaya, V.A. Zakharov, A.V. Golovin, T.B. Mikenas, Macromol. Chem. Phys. 200 (1999) 1434–1438.

[46] N.V. Semikolenova, W.-H. Sun, I.E. Soshnikov, M.A. Matsko, O.V. Kolesova, V.A. Zakharov, K.P. Bryliakov, ACS Catal. 7 (2017) 2868–2877.